The Chemistry of Isomers of Icosaborane(26), $B_{20}H_{26}$: Synthesis and Nuclear Magnetic Resonance Study of Various Isomers of Platinaheni-cosaboranes and Diplatinadocosaboranes, and the *X*-Ray Crystal and Molecular Structures of 7,7-Bis(dimethylphenylphosphine)-*nido*-7-platinaundecaborane and 4-(2′-*nido*-Decaboranyl)-7,7-bis(dimethyl-phenylphosphine)-*nido*-7-platinaundecaborane

By **Simon K. Boocock, Norman N. Greenwood,* John D. Kennedy, Walter S. McDonald,** and **John Staves,** Department of Inorganic and Structural Chemistry, University of Leeds, Leeds LS2 9JT

An improved synthesis of the known compound $[(PMe_2Ph)_2(PtB_{10}H_{12})]$ has been developed by deprotonation of $B_{10}H_{14}$ with *NNN′N′*-tetramethylnaphthalene-1,8-diamine followed by treatment with *cis*-$[PtCl_2(PMe_2Ph)_2]$. This reaction has been applied to the 2,2′, 2,6′, and 1,5′ isomers of $(B_{10}H_{13})_2$ to prepare various isomeric platina-henicosaborane clusters $[(PMe_2Ph)_2(PtB_{10}H_{11}{-}B_{10}H_{13})]$ which differ either in the position of the *conjuncto*-linkage or the site of the platinum atom in the cluster. Appropriate modification of the reaction stoicheiometry in the case of 2,2′-$(B_{10}H_{13})_2$ led to the isolation of *cisoid* and *transoid* diplatinadocosaboranes $[\{(PMe_2Ph)_2(PtB_{10}H_{11})\}_2]$. The *X*-ray crystal structure of $[(PMe_2Ph)_2(PtB_{10}H_{12})]$ showed it to contain a platinaundecaborane cluster in which the tetrahapto $B_{10}H_{12}$ group is twisted by *ca.* 20° with respect to the PtP_2 plane. Similarly, the molecular structure of the isomer of $[(PMe_2Ph)_2Pt(\eta^4\text{-}B_{10}H_{11}{-}B_{10}H_{13})]$ obtained from 2,2′-$(B_{10}H_{13})_2$ is distorted by a twist of *ca.* 8°. A detailed n.m.r. study of a number of these clusters has been made, using the resonances of ^1H, ^{11}B, ^{31}P, and ^{195}Pt. In addition to permitting structural assignments, the data reveal a novel mutual pseudo-rotation of the η^4-$B_{10}H_{11}X$ group (X = H or $B_{10}H_{13}$) and the $(PMe_2Ph)_2$ grouping about the central Pt atom. For $[(PMe_2Ph)_2(PtB_{10}H_{12})]$ the two sets of ^1H-$\{^{31}P\}$ methyl resonances at 100 MHz coalesce at 71.5 °C with an implied activation energy $\Delta G^{\ddagger}$ of 79 ± 5 kJ mol^{-1} for the fluxional process. Similar activation energies were deduced for the various isomers of $[(PMe_2Ph)_2(PtB_{20}H_{24})]$.

SINCE the initial discovery [1] of icosaborane(26), $B_{20}H_{26}$, as an impurity in technical-grade *nido*-decaborane, a substantial amount of synthetic and structural work has been reported.[2-8] The compound has the bi(*nido*-decaboranyl) structure, $(B_{10}H_{13})_2$, and to date seven of its possible eleven geometrically distinct isomers, *viz.* 1,2′-, 1,5′-, 2,2′-, 2,5′-, 2,6′-, 6,6′-, and 5,5′- (or 5,7′)-$(B_{10}H_{13})_2$, have been individually isolated and identified either by *X*-ray crystallography [4-6] or by high-resolution n.m.r. spectroscopy.[3,8] The chemistry of these interesting species however remains largely unexplored, and we therefore now report the preparation of various bis-(dimethylphenylphosphine)platinum derivatives of the 2,2′- and 2,6′-$(B_{10}H_{13})_2$ isomers together with some related work on the 1,5′ isomer. This work includes the crystal and molecular structure of the $Pt(PMe_2Ph)_2$ derivative of 2,2′-$(B_{10}H_{13})_2$ together with the analogous derivative of $B_{10}H_{14}$ itself for comparison. Some preliminary and incidental aspects have been presented elsewhere,[9,10] and this work also forms part of a wider programme to investigate structural implications of metalloborane chemistry using platinum as a model metal.[11-14] In this paper we use the conventional I.U.P.A.C.-recommended [15] numbering systems [structures (I) and (II)] for the constituent atoms of the eleven- and ten-vertex clusters discussed. In these systems the addition of an atom as an additional vertex to the ten-vertex cluster changes the numbering of the other cluster atoms, but reference to (I) and (II) will clarify the relationships in each case.

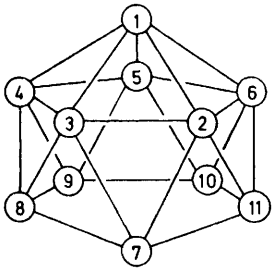

(Ia)

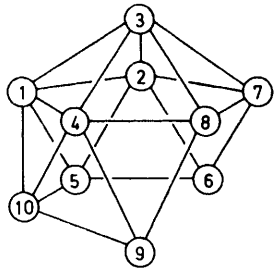

(IIa)

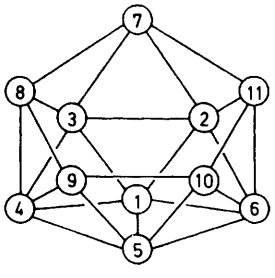

(Ib)

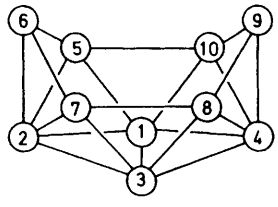

(IIb)

RESULTS AND DISCUSSION

Preparative Work and N.M.R. Parameters.—In our work to derivatise the isomers of $(B_{10}H_{13})_2$ we have initially chosen as our models reactions that are already known to occur with *nido*-decaborane itself in high yield (based on decaborane) and under mild conditions. Of these, the first preparations of 7,7′-bis(phosphine)-*nido*-7-platinaundecaboranes were reported some time ago: [16] the syntheses were effected *via* initial deproton-

ation of decaborane [equation (1)] followed by reaction with bis(phosphine)platinum dihalide [equation (2)] but the yield was moderate and in any event was limited to a

$$B_{10}H_{14} + KH \longrightarrow B_{10}H_{13}^- + K^+ + H_2 \quad (1)$$

$$2K[B_{10}H_{13}] + cis\text{-}[PtCl_2(PR_3)_2] \longrightarrow [(PR_3)_2(PtB_{10}H_{12})] + B_{10}H_{14} + 2KCl \quad (2)$$

maximum of 50% by the stoicheiometry of equation (2). We have therefore examined an analogous reaction using two equivalents of the weak nucleophile *NNN'N'*-tetramethylnaphthalene-1,8-diamine as base and this has resulted in good yields of the isolated platinaundecaborane in small-scale syntheses [equation (3)]. In-

$$B_{10}H_{14} + cis\text{-}[PtCl_2(PMe_2Ph)_2] + 2C_{10}H_6(NMe_2)_2 \longrightarrow [(PMe_2Ph)_2(PtB_{10}H_{12})] + 2[C_{10}H_6(NMe_2)(NHMe_2)]^+ + 2Cl^- \quad (3)$$

dependent work on the utility of tetramethylnaphthalenediamine as a deprotonating agent for polyhedral boranes has recently been reported elsewhere.[17]

7,7-Bis(dimethylphenylphosphine)-*nido*-7-platinaundecaborane, $[(PMe_2Ph)_2(PtB_{10}H_{12})]$ [numbering system as in structure (I)], is a bright yellow air-stable solid [m.p. 197—199 °C (decomp.)] which readily yielded crystals suitable for single-crystal *X*-ray diffraction analysis. The structure (Figure 1), which is discussed in

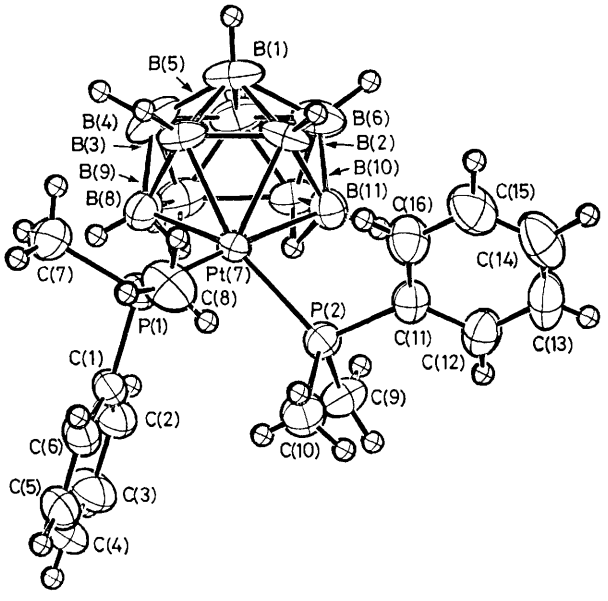

FIGURE 1 ORTEP drawing showing the molecular structure and atom numbering of $[(PMe_2Ph)_2(PtB_{10}H_{12})]$

more detail below, can in the first instance be regarded as derived from that of *nido*-decaborane by the replacement of two bridging hydrogen atoms by two three-centre bonds to the *cis*-$Pt(PMe_2Ph)_2$ moiety. The formal platinum(II) tetragonal bonding plane then involves these two three-centre bonds and the two phosphorus atoms. The ^{11}B and ^1H n.m.r. behaviour of the effective *nido*-decaboranyl $B_{10}H_{12}^{2-}$ ligand in this compound has been reported and discussed elsewhere;[18] there is a general deshielding of the skeletal ^{11}B and ^1H nuclei upon the conversion of $B_{10}H_{14}$ into the platinaundecaborane, and in particular the B(2,4) nuclei [numbering as in structure (II)] undergo a decrease in shielding of 8.2 p.p.m. upon the formation of the platinum compound. Other previously unreported n.m.r. parameters are summarised in Table 1. The ^{31}P-{^1H} n.m.r.

TABLE 1

Proton and phosphorus-31 n.m.r. parameters of the *P*-methyl groups in [7,7-$(PMe_2Ph)_2$-*nido*-7-$PtB_{10}H_{12}$] [a]

$\delta(^1H)$/p.p.m.[b]	A + 1.86 ± 0.02	B + 1.70 ± 0.02
$N(^{31}P-^1H)$/Hz [c]	A − 9.5 ± 0.2	B − 10.9 ± 0.2
$^3J(^{195}Pt-^1H)$/Hz	A + 25.2 ± 0.2	B + 24.8 ± 0.2
$\delta(^{31}P)$/p.p.m.[d]	+ 1.3 ± 0.5	
$^1J(^{195}Pt-^{31}P)$/Hz	+ 2 534 ± 4	
$\Xi(^{195}Pt)$ [e]	21 379 830 ± 20	

[a] In CD_2Cl_2 at 21 °C unless otherwise specified; A and B specify the chemically independent *P*-methyl groups that arise from the prochirality of the 7-platina position. [b] To low field (high frequency) of $SiMe_4$. [c] $N = {}^2J(^{31}P-^1H) + {}^4J(^{31}P-^1H)$. [d] To low field (high frequency) of 85% H_3PO_4. [e] From ^1H-{^{195}Pt} experiments conducted in collaboration with Dr. W. McFarlane; see also ref. 18.

spectrum at ambient temperature consists of a broad central singlet flanked by 'satellites' arising from coupling to ^{195}Pt; on cooling, 'thermal decoupling' of the ^{11}B and ^{10}B quadrupolar nuclei occurs,[19] and the lines sharpen but as expected reveal no fine structure. The two *P*-methyl groups on each of the two equivalent PMe_2Ph ligands differ chemically since they are adjacent to a prochiral centre and as such exhibit two independent sets of lines in their ambient-temperature ^1H n.m.r. spectra (*e.g.* Figure 2). Each set of lines takes the form of a central agglomerate of resonances flanked by similar satellite lines arising from those molecules containing ^{195}Pt. The shapes of the agglomerates resemble the X parts of $[AX_n]_2$ spectra [20] (A = ^{31}P, X = ^1H), although actually the spin system will be $[AX_3Y_3]_2$, in which $J(XY)$ [= $^4J(^1H-C-P-C-^1H)$] will be small, and in addition, couplings to ^{11}B, ^{10}B, and ^1H(borane and aromatic hydrocarbon) will also be involved. In the resonance envelopes, however, the '*N*' lines are readily distinguished and the shape of the additional intensity [20] suggests a value for $^2J(^{31}P-Pt-^{31}P)$ of two or three tens of Hz, consistent with the *cis* stereochemistry. The relative sign information determined by ^1H-{^{31}P} and ^1H-{^{195}Pt} selective double-irradiation experiments is also as expected, but it is interesting to note a general *broadening* of the *P*-methyl ^1H resonances, which particularly affects the central 'non-*N*-line' parts of the resonance envelope, upon simultaneous ^{11}B irradiation. It is also of interest to note that, on heating the sample, the ^1H resonances coalesce indicating a fluxional process as discussed in more detail below.

The reaction of equation (3) when applied to the icosaborane 2,2'-$(B_{10}H_{13})_2$ also yielded a yellow crystalline platinaborane product [m.p. 194—199 °C (decomp.)] in good yield, and analytical and molecular-weight data indicated the formation of a mono[bis(dimethylphenyl-

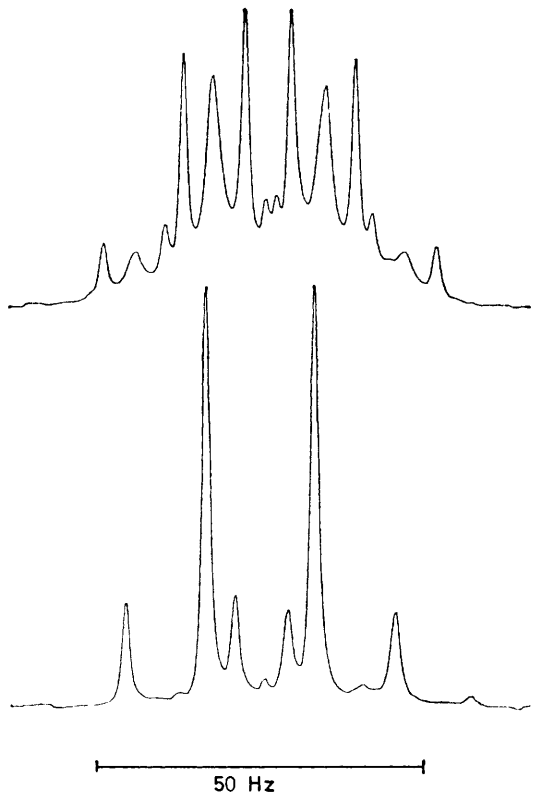

FIGURE 2 100-MHz Proton n.m.r. spectra of the *P*-methyl resonances in $[(PMe_2Ph)_2(PtB_{10}H_{12})]$ in CD_2Cl_2 solution at 21 °C: upper trace, normal spectrum; lower trace (at reduced spectrometer gain), spectrum with ^{31}P(broad-band noise) decoupling

phosphine)platinum] derivative of the icosaborane as in (4). The 32-MHz ^{11}B n.m.r. spectra in the low-field

$$2,2'\text{-}(B_{10}H_{13})_2 + cis\text{-}[PtCl_2(PMe_2Ph)_2] + 2C_{10}H_6(NMe_2)_2 \longrightarrow [(PMe_2Ph)_2(PtB_{20}H_{24})] + 2[C_{10}H_6(NMe_2)(NHMe_2)]^+ + 2Cl^- \quad (4)$$

basal and 'hinge' boron region [$\delta(^{11}B)$ *ca.* +20 to −10 p.p.m.] were similar to a superposition of the spectra of $2,2'\text{-}(B_{10}H_{13})_2$ and $[(PMe_2Ph)_2(PtB_{10}H_{12})]$, although somewhat broader as would be expected from a slower rotational diffusion arising out of a larger molecular bulk.[19] The high-field apical region (δ −20 to −40 p.p.m.) showed four resonances of equal intensity at $\delta(^{11}B)$ = −22.5, −24.9, −32.5, and −35.0 p.p.m. of which those at −22.5 and −32.5 p.p.m. remained singlets in the absence of ^1H(broad-band noise) decoupling. This is clearly consistent with a $2,2'\text{-}(B_{10}H_{13})_2$ structure in which one of the *nido*-decaboranyl clusters has been converted into a *nido*-7-platinaundecaboranyl cluster with the expected concomitant deshielding [18] of *ca.* 10 p.p.m. in the apical ^{11}B resonances of the cage concerned. This structural conclusion is confirmed by the results of a single-crystal *X*-ray diffraction analysis (Figure 3) which is discussed in more detail below, but which shows that the gross structure is that of 7,7-bis(dimethylphenylphosphine)-*nido*-7-platinaundecaborane (Figure 1), but now with a pendant 4-(2′-*nido*-decaboranyl) cluster bonded to it, *i.e.* the compound is 4-(2′-*nido*-decaboranyl)-7,7-bis(dimethylphenylphosphine)-*nido*-7-platinaundecaborane, $[4\text{-}(2'\text{-}B_{10}H_{13})\text{-}7,7\text{-}(PMe_2Ph)_2\text{-}7\text{-}PtB_{10}H_{11}]$.

Other n.m.r. features are readily interpretable in terms of this structure. The $^1H\text{-}\{^{11}B\}$ spectra of the borane cluster protons at 100 MHz contain in general too many overlapping or partially overlapping peaks for satisfactory analysis, but in the bridging region at $\delta(^1H) <$ *ca.* −1 p.p.m. they exhibited peaks at $\delta(^1H)$ = −1.61, −1.83, and −2.67 p.p.m. ($CDCl_3$ solution)

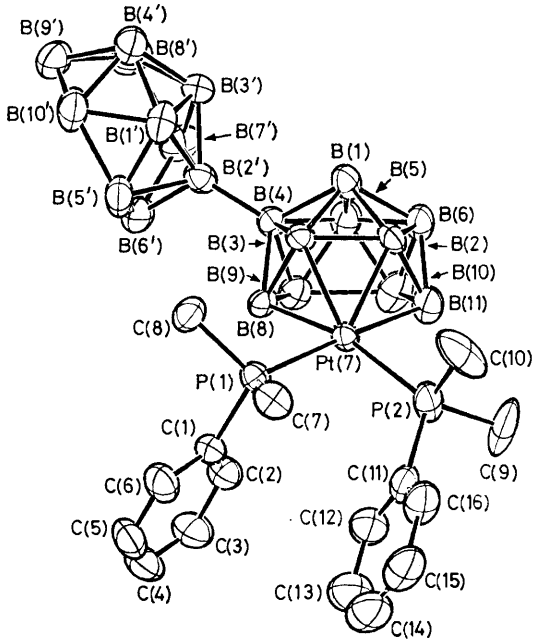

FIGURE 3 ORTEP drawing showing the molecular structure and atom numbering of $[(PMe_2Ph)_2(PtB_{20}H_{24})]$ from $2,2'\text{-}(B_{10}H_{13})_2$. Both enantiomers are contained in the unit cell

[−1.15, −1.51, −2.18, and −2.53 p.p.m. (C_6D_6 solution)] of relative intensities 1 : 1 : 4 (and 1 : 1 : 2 : 2) respectively, again consistent with the structure and readily assignable between the two clusters on the basis of the established shielding behaviour [6,18] of the *nido*-decaboranyl and *nido*-7-platinaundecaboranyl clusters. At ambient temperatures the $^{31}P\text{-}\{^1H$(broad-band noise)$\}$ spectrum is a broad singlet flanked by ^{195}Pt satellites, as for $[(PMe_2Ph)_2(PtB_{10}H_{12})]$, but at low temperatures fine structure is observed (*e.g.* Figure 4). In this low-temperature spectrum the resonance frequencies for the two inequivalent ^{31}P nuclei are nearly degenerate so that the central resonance is effectively a singlet, but there are slight differences in the two couplings $^1J(^{195}Pt\text{–}^{31}P)$ which result in two AB sub-spectra centred at $\nu(^{31}P)_{mean} \pm \frac{1}{2}{}^1J(^{195}Pt\text{–}^{31}P)_{mean}$; straightforward AB spectral analysis yields the parameters summarised in Table 2, and the coupling $^2J(^{31}P\text{–}Pt\text{–}^{31}P)$ of *ca.* 30 Hz is similar to that which may be estimated for the unsubstituted platinaundecaborane on the basis of the shape of the ^1H resonances

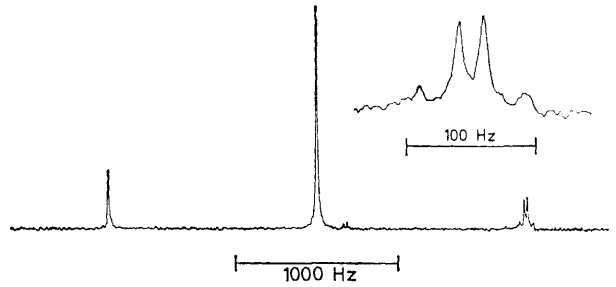

FIGURE 4 40-MHz ^{31}P-{^{1}H(broad-band noise)} n.m.r. spectrum of [4-(6′-$B_{10}H_{13}$)-7,7′-$(PMe_2Ph)_2$-*nido*-7-$PtB_{10}H_{11}$] in CD_2Cl_2 solution at −42 °C. The upper trace is that of the high-field (low-frequency) ^{195}Pt satellite subspectrum at an increased scale expansion. The corresponding spectrum for the 4-(2′-$B_{10}H_{13}$) isomer is similar

in the *P*-methyl groups. It is worth [21] re-emphasising at this point that the splitting effects in the ^{31}P spectra observed here do not arise from ^{1}H coupling, since the effects of this are eliminated by efficient ^{1}H(broad-band noise) irradiation, and also that the origin of this fine structure differs from that observed for more complex, but more symmetrical, phosphineplatinaborane spin

TABLE 2

N.m.r. parameters for the *P*-methyl groups in the platinahenicosaboranes [4-(2′-$B_{10}H_{13}$)-7,7-$(PMe_2Ph)_2$-*nido*-7-$PtB_{10}H_{11}$] and [4-(6′-$B_{10}H_{13}$)-7,7-$(PMe_2Ph)_2$-*nido*-7-$PtB_{10}H_{11}$] [a]

		4-(2′-$B_{10}H_{13}$) compound	4-(6′-$B_{10}H_{13}$) compound
$\delta(^{1}H)$/p.p.m. [b]	A	+1.90	+1.93
	B	+1.80	+1.83
	C	+1.75	+1.77
	D	+1.53	+1.63
$^{3}J(^{195}Pt-^{1}H)$/Hz [c]	A	+24.4	+24.9
	B	+24.4	+24.9
	C	+25.4	+25.0
	D	+24.4	+24.9
$\delta(^{31}P)$/p.p.m. [d]	E	+0.6	+1.3 [e]
	F	+0.7	+1.2 [e]
$^{1}J(^{195}Pt-^{31}P)$/Hz [e]	E	+2 568 ± 10	+2 548 ± 10
	F	+2 498 ± 10	+2 510 ± 10
$\|^{2}J(^{31}P-^{31}P)\|$/Hz [e]		31 ± 1	30 ± 1

[a] In CD_2Cl_2 at 21 °C unless otherwise designated. Letters A—F distinguish chemically different nuclei. [b] ±0.02 p.p.m. to high frequency (low field) of $SiMe_4$. [c] ±0.2 Hz. [d] ±0.5 p.p.m. to high frequency (low field) of 85% H_3PO_4. [e] At −63 °C.

systems, such as that [14] in [6,6,9,9-$(PMe_2Ph)_4$-*arachno*-6,9-$Pt_2B_8H_{10}$]. Also summarised in Table 2 are the ^{1}H data for the *P*-methyl groups. The four methyl groups in this compound are now *all* mutually inequivalent and there is an effective $[AW_3X_3][BY_3Z_3]$ spin system (A,B = ^{31}P; W,X,Y,Z = ^{1}H) if boron and longer-range ^{1}H couplings are disregarded. In accord with this, four ^{1}H resonance patterns are observed, of which each approximates in appearance to the X part of an $[AX_n]_2$ system and is also flanked by ^{195}Pt satellites. These are readily distinguishable with the aid of ^{31}P-(broad-band noise) decoupling (Figure 5). On warming the sample these ^{1}H resonances coalesce in pairs due to intramolecular pseudo-rotation about the platinum atom as discussed below.

We have also examined the behaviour of two other $(B_{10}H_{13})_2$ isomers under the conditions of reaction (4). The isomer 2,6′-$(B_{10}H_{13})_2$ yields two metalloborane products which may be separated chromatographically. One of these is identifiable as [7,7-$(PMe_2Ph)_2$-7-$PtB_{10}H_{12}$] and the second as a [$(PMe_2Ph)_2(PtB_{20}H_{24})$] species: the

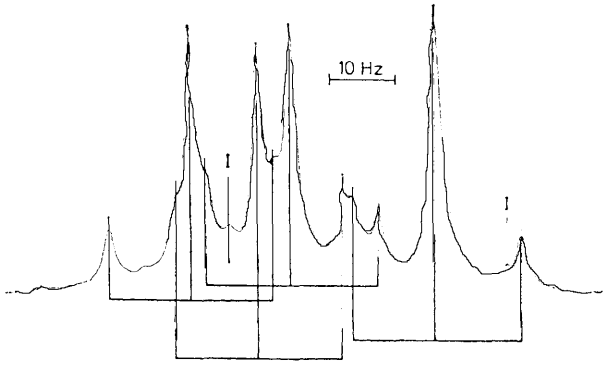

FIGURE 5 100-MHz ^{1}H-{^{31}P(broad-band noise)} n.m.r. spectrum of the *P*-methyl resonances in [4-(2′-$B_{10}H_{13}$)-7,7-$(PMe_2Ph)_2$-*nido*-7-$PtB_{10}H_{11}$] in CD_2Cl_2 solution at 21 °C. Peaks I are from impurities, and the four *P*-methyl singlet resonances, each flanked by ' satellites ' arising from coupling $|^{3}J(^{195}Pt-^{1}H)| = ca.$ 25 Hz (see Table 2), are readily apparent. The corresponding spectrum for the 4-(6′-$B_{10}H_{13}$) isomer is similar

^{1}H and ^{31}P n.m.r. properties of the PMe_2Ph groups (Table 2) are similar to those of [4-(2′-$B_{10}H_{13}$)-7,7-$(PMe_2Ph)_2$-7-$PtB_{10}H_{11}$], exhibiting four *P*-methyl resonances in the ^{1}H spectrum and two near-equivalent resonances in the ^{31}P spectrum, and the ^{11}B n.m.r. spectrum in the region $\delta(^{11}B) = ca.$ +20 to −10 p.p.m. is also similar to that described for the 4-(2′-$B_{10}H_{13}$)-substituted species. In the high-field apical region [$\delta(^{11}B)$ −20 to −40 p.p.m.], however, four resonances may be distinguished which by ' partially relaxed ' Fourier-transform spectroscopy [22,23] are revealed as three doublets and a singlet (Figure 6). Of these the singlet due to the apical boron atom involved in the *conjuncto*-linkage is one of the two lower-field resonances and thus this compound results from the attachment of the $Pt(PMe_2Ph)_2$ moiety to the 2-($B_{10}H_{13}$) residue of 2,6′-$(B_{10}H_{13})_2$. The product is therefore 4-(6′-*nido*-decaboranyl)-7,7-bis(dimethylphenylphosphine)-*nido*-7-platinaundecaborane [schematic structure (IIIa)] which will coexist as a racemate with its 6-(6′-*nido*-decaboranyl) enantiomorph [see schematic structure (IIIb)]; the bright yellow compound has m.p. 201—211 °C (decomp.). Interestingly we have not so far been able to detect significant quantities of any other [$(PMe_2Ph)_2$-$(PtB_{20}H_{24})$] isomers, such as, in particular, the expected 8-(2′-*nido*-decaboranyl) species, in this product mixture. The formation of this last compound would not be favoured sterically, but its absence together with the incidence of [$(PMe_2Ph)_2(PtB_{10}H_{12})$] may also indicate a preferential cleavage of the *conjuncto*-B–B bond when

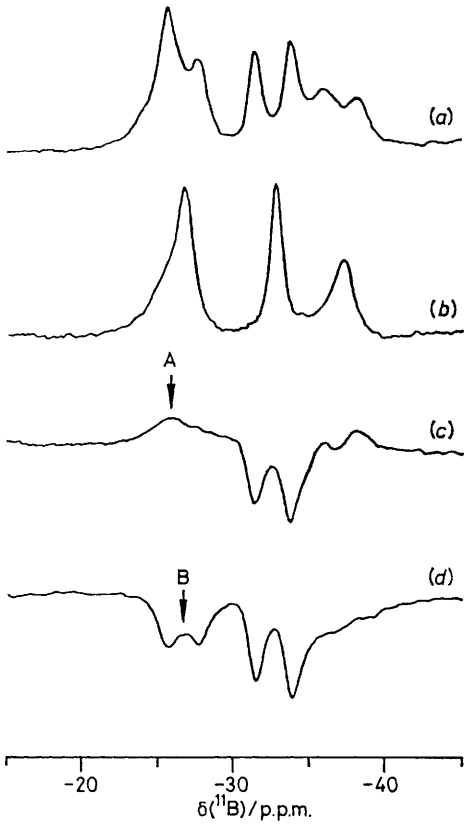

FIGURE 6 64-MHz Boron-11 n.m.r. spectra of the B(4)B(6)B(2')-B(4') region of [4-(6'-$B_{10}H_{13}$)-7,7-*nido*-7-$PtB_{10}H_{11}$] in CD_2Cl_2 solution at 35 °C: (*a*) normal ^{11}B spectrum; (*b*) ^{11}B spectrum with ^1H(broad-band noise) decoupling; (*c*) and (*d*) 'partially relaxed' ^{11}B spectra obtained using the 180—τ—90° pulse sequence with τ = 4 (*c*) and 2 ms (*d*). These spectra show that the resonances at $\delta(^{11}B)$ = *ca.* −26 p.p.m. consist of a singlet A at δ (^{11}B) = −25.7 p.p.m., with T_1 (^{11}B) = *ca.* 3 ms, and a doublet centred at B with $\delta(^{11}B)$ = −26.7 p.p.m., ^1J (^{11}B–^1H) = *ca.* 130 Hz, and T_1 (^{11}B) = *ca.* 6 ms

one of the boron atoms involved in this linkage [in this case the 6' boron atom of 2,6'-$(B_{10}H_{13})_2$] takes part in the incipient metal–boron bond formation.

This hypothesis can also be invoked to account for the behaviour of 1,5'-$(B_{10}H_{13})_2$ when this is treated under the conditions of reaction (4). Chromatographic separation of the products again yields [$(PMe_2Ph)_2(PtB_{10}H_{12})$] plus three species tentatively identified as *nido*-decaboranyl-bis(phosphine)-*nido*-platinaundecaborane isomers. We have so far only been able to achieve a partial separation of these three, but it would be reasonable to suppose that they would be the 1-(5'-*nido*-decaboranyl)/1-(7'-*nido*-decaboranyl) racemate, the 5-(5'-*nido*-decaboranyl)/5-(7'-*nido*-decaboranyl) racemate and the 9-(1'-*nido*-decaboranyl)/10-(1'-*nido*-decaboranyl) racemate, with the formation of the fourth possibility, the 3-(1'-*nido*-decaboranyl)/2-(1'-*nido*-decaboranyl) racemate, being sterically unfavoured and/or resulting in *conjuncto*-B–B bond cleavage and production of [$(PMe_2Ph)_2(PtB_{10}H_{12})$].

An extension of reaction (4) is to double the amounts of base and bis(phosphine)platinum dichloride to produce a bi(*nido*-7-platinaundecaboranyl) compound as in equation (5). We have examined this reaction using

$$(B_{10}H_{13})_2 + 2[PtCl_2(PMe_2Ph)_2] + 4C_{10}H_6(NMe_2)_2 \longrightarrow [(PMe_2Ph)_4(PtB_{10}H_{11})_2] + 4[C_{10}H_6(NMe_2)(NHMe_2)]Cl \quad (5)$$

2,2'-$(B_{10}H_{13})_2$ and have found that three products are formed which may be separated chromatographically.

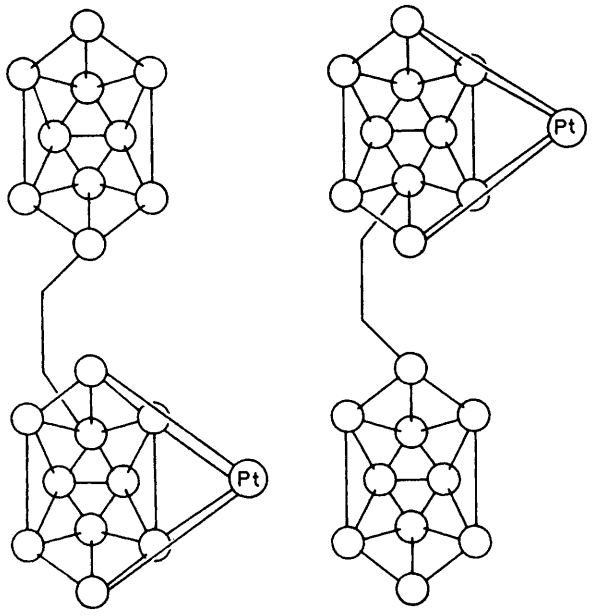

(IIIa) (IIIb)

One of these is the 4-(2'-*nido*-decaboranyl)-*nido*-7-platinaundecaborane discussed above, and the analytical and molecular-weight data for the other two, which are brilliant yellow compounds [m.p. 175—180 (decomp.) and 158—170 °C (decomp.)], suggest species with the bi[7,7-bis(dimethylphenylphosphine)-*nido*-7-platinaundecaboranyl] formulation. Consistent with this, both exhibit four *P*-methyl ^1H resonances and two near-equivalent ^{31}P resonances in their n.m.r. spectra and their ^{11}B spectra exhibit similar maxima to those [18] of [$(PMe_2Ph)_2(PtB_{10}H_{12})$] but the lines are very broad indeed. The two components are therefore presumably the *cisoid* compound 4,6'-[$(PMe_2Ph)_2(PtB_{10}H_{11})$]$_2$ [schematic structure (IV)] and the *transoid* compound 4,4'-[$(PMe_2Ph)_2(PtB_{10}H_{11})$]$_2$ [schematic structure (V)]. The 4,6' compound will be structurally unique, but the 4,4' will be paired enantiomerically with the 6,6' isomer. However, these two structures cannot be distinguished spectroscopically in the achiral solvents that we have been able to use, and we have not yet been able to grow single crystals suitable for *X*-ray diffraction analysis.

Molecular Structures of [$(PMe_2Ph)_2(PtB_{10}H_{12})$] *and* [4-(2'-$B_{10}H_{13}$)-7,7-$(PMe_2Ph)_2$-7-$PtB_{10}H_{11}$].—An ORTEP drawing of the molecular structure of the *nido*-7-platinaundecaborane is in Figure 1, atomic co-ordinates are in the Experimental section, and selected interatomic distances and angles are in Tables 3 and 4 respectively.

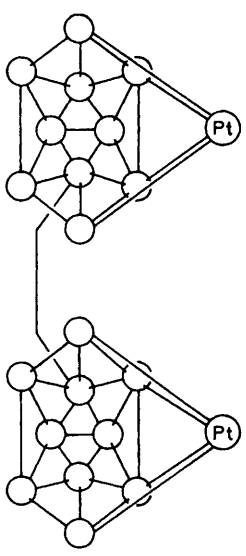

(IV)

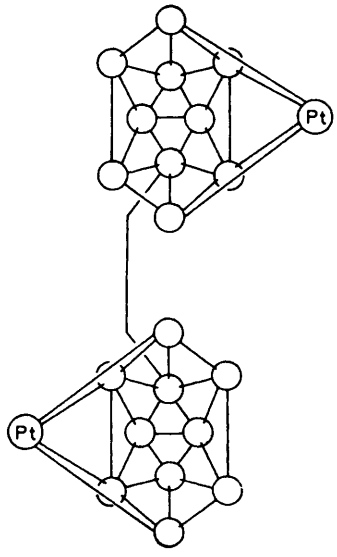

(V)

Also included in Table 3 for comparison are equivalent data for related compounds; horizontal rows compare corresponding distances in the various ten-boron clusters.

The gross structure of the metallaborane unit is seen to be that of a *nido*-eleven-vertex cluster, and as such is similar to those in related species such as $B_{11}H_{13}^{2-}$,[24] $[Ni(B_{10}H_{12})_2]^{2-}$,[25] and $[Me_2TlB_{10}H_{12}]^-$,[26] *etc.* The compound may be regarded as a metal complex of the η^4-$B_{10}H_{12}^{2-}$ ligand or as a *nido*-metallaundecaborane species.

TABLE 4

Selected angles (°) between interatomic vectors, for [7,7-$(PMe_2Ph)_2$-7-$PtB_{10}H_{12}$], with estimated standard deviations in parentheses *

P(1)–Pt(7)–P(2)	95.4(1)		
P(1)–Pt(7)–B(2)	138.1(2)	P(2)–Pt(7)–B(3)	162.4(1)
P(1)–Pt(7)–B(3)	98.9(1)	P(2)–Pt(7)–B(2)	114.1(2)
P(1)–Pt(7)–B(8)	89.6(2)	P(2)–Pt(7)–B(11)	82.7(1)
P(1)–Pt(7)–B(11)	176.2(1)	P(2)–Pt(7)–B(8)	144.3(1)
B(2)–Pt(7)–B(3)	48.4(2)		
B(2)–Pt(7)–B(8)	83.2(2)	B(3)–Pt(7)–B(11)	83.5(2)
B(2)–Pt(7)–B(11)	45.6(2)	B(3)–Pt(7)–B(8)	46.4(2)
B(8)–Pt(7)–B(11)	90.1(2)		

* The two columns compare pairs of angles which would be identical if the molecule had C_s symmetry about the Pt(7)B(1)-B(5) plane.

In this *nido*-cluster the Pt atom occupies one of the basal (open-face) positions, and, as expected, the Pt–B and B–B distances in the open face are a few pm longer than the other Pt–B and B–B distances in the molecule, which all fall within normal ranges.[14] All hydrogen

TABLE 3

Interatomic distances (pm) for [7,7-$(PMe_2Ph)_2$-7-$PtB_{10}H_{12}$] and related compounds, with estimated standard deviations in parentheses [a]

	$[(PMe_2Ph)_2PtB_{10}H_{12}]$			$B_{10}H_{14}$ [b]	$[Ni(B_{10}H_{12})_2]^{2-}$ [c]		$[Me_2TlB_{10}H_{12}]^-$ [d]	
(*a*) From the platinum atom								
Pt(7)–P(1)	230.9(1)	Pt(7)–P(2)	233.7(1)					
Pt(7)–B(2)	221.4(5)	Pt(7)–B(3)	222.5(5)		211(1)	218(1)	261(2)	251(2)
Pt(7)–B(11)	230.1(6)	Pt(7)–B(8)	227.9(6)		224(1)	222(1)	277(2)	276(2)
(*b*) Boron–boron								
B(1)–B(2)	176.5(9)	B(1)–B(3)	175.0(9)	175.4(4)	181(2)	177(2)	177(3)	181(3)
B(1)–B(4)	173.3(10)	B(1)–B(6)	177.4(9)	178.2(5), 177.4(5)	177(2)	180(2)	175(3)	180(3)
B(1)–B(5)	175.7(9)			177.2(6)	180(2)		176(3)	
B(2)–B(3)	181.8(8)			197.3(4)	187(2)		197(3)	
B(2)–B(6)	176.2(9)	B(3)–B(4)	176.0(9)	178.5(5), 178.7(5)	181(2)	177(2)	178(3)	180(3)
B(2)–B(11)	175.0(8)	B(3)–B(8)	177.5(8)	178.8(5), 176.2(5)	175(2)	177(2)	174(3)	170(3)
B(4)–B(5)	176.7(9)	B(6)–B(5)	175.9(9)	178.2(5), 177.4(5)	177(2)	180(2)	175(3)	180(3)
B(4)–B(8)	174.6(9)	B(6)–B(11)	174.9(8)	171.5(4)	175(2)	177(2)	172(3)	171(3)
B(4)–B(9)	177.7(9)	B(6)–B(10)	177.1(8)	178.5(3), 178.7(5)	177(2)	174(2)	175(3)	178(3)
B(5)–B(9)	175.6(9)	B(5)–B(10)	173.7(8)	175.8(4), 175.4(4)	173(2)	177(2)	179(3)	175(3)
B(8)–B(9)	180.9(9)	B(10)–B(11)	184.1(8)	178.8(5), 176.2(5)	183(2)	184(2)	177(3)	179(3)
B(9)–B(10)	197.6(9)			197.3(4)	197(2)		206(3)	
(*c*) Boron–hydrogen								
B(1)–H(1)	106(6)							
B(2)–H(2)	118(5)	B(3)–H(3)	110(6)					
B(4)–H(4)	112(6)	B(6)–H(6)	114(5)					
B(5)–H(5)	104(5)							
B(8)–H(8)	95(5)	B(11)–H(11)	97(5)					
B(9)–H(9)	110(5)	B(10)–H(10)	112(4)					
B(8)–H(8,9)	125(4)	B(11)–H(10,11)	122(5)					
B(9)–H(8,9)	121(4)	B(10)–H(10,11)	129(5)					
(*d*) Other								
P–C	180.3—182.6(7) (average 181.4)							
C–C	135.5—139.1(8) (average 137.8)							
C–H	80—109(8) (average 94)							

[a] The first two columns compare pairs of distances that would be identical if the molecule had C_s symmetry about the Pt(7)B(1)B(5) plane. [b] From neutron diffraction on $B_{10}D_{14}$; A. Tippe and W. C. Hamilton, *Inorg. Chem.*, 1969, **8**, 464. [c] From *X*-Ray diffraction; ref. 25. [d] From *X*-Ray diffraction; ref. 26.

atoms were located and included in the refinement. The validity of the H-atom refinement is supported by the satisfactory convergence, the physically reasonable thermal parameters, and the chemically reasonable bond lengths (95—118 pm for terminal B–H, 121—129 pm for bridging BH). The incidence of bridging H atoms in the (8,9) and (10,11) positions is consistent with a *nido*-cluster electron count, and also confirms the compound as a derivative of *nido*-decaborane in which the other two bridging H atoms in $B_{10}H_{14}$ have been in the first instance formally replaced by two two-electron three-centre bonds to the $Pt(PMe_2Ph)_2$ moiety [*viz.* Pt(7)B(3)B(8) and Pt(7)B(2)B(11)]. The B(2)–B(11) and B(3)–B(8) distances in the metallaborane indicate that some contraction has occurred upon the replacement of these bridging H atoms by bonds to Pt, as also noted [14] for η^3-borane–metal bonding in species such as $[(PMe_2Ph)_2(PtB_8H_{12})]$, but these changes are small. By contrast, the B(2)–B(3) distance is markedly less (15 pm) than the corresponding B(5)–B(10) distance in $B_{10}H_{14}$. A similar contraction also occurs in $[Ni(B_{10}H_{12})_2]^{2-}$ (10 pm),[25] but in the main-group derivative $[Me_2TlB_{10}H_{12}]^-$ the distance is the same as in unsubstituted $B_{10}H_{14}$.[26] This suggests that the transition-metal derivatives have enhanced M(7)B(2)-B(3) three-centre bonding contributions which probably occur *via* additional *d*-orbital participation. This is to some extent supported by the ^{11}B n.m.r. shielding behaviour in the nickel and platinum compounds which is substantially different from that in $B_{10}H_{14}$ for these particular positions;[18,27] in the main-group derivatives such as $[Me_2TlB_{10}H_{12}]^-$ and $[MeHgB_{10}H_{12}]^-$, by contrast, the shielding behaviour in this region appears to be quite similar to that of $B_{10}H_{14}$.[28]

Comparison of horizontal rows in the first two columns of Table 3 indicates that the symmetry of the platinaundecaborane cage approximates to C_s, the only statistically significant deviations being possibly those between each of the B(1)B(4)/B(1)B(6) and B(8)B(9)/B(10)B(11) pairs, which may be associated with the distortion about the Pt(7) atom apparent from the positions of the two phosphine ligands. The positions of the two P atoms in fact introduce a substantial deviation from C_s symmetry. Although within the normal range [14,29–32] for this type of compound, the two Pt–P bond lengths differ significantly, and the angular comparisons (Table 4) show a considerable twist deviation from idealised geometry; this last is presumably the source of the inequality in the Pt–P distances. This is illustrated in Figure 7, which is a projection, viewed in the Pt(7)P(1)P(2) plane, of the Pt and its circumjacent bonded atoms. Here it can be seen that the platinum tetragonal bonding plane, as defined by the Pt(7)P(1)P(2) plane, is at an angle of *ca.* 20° to that expected for an undistorted dsp^2 hybridisation involving the two-electron three-centre Pt(7)B(2)B(11) and Pt(7)B(3)B(8) bonds directed towards the midpoints of B(2)B(11) and B(3)B(8). We ascribe this 'twist' distortion to crystal-packing constraints rather than electronically dictated asymmetric bonding as possibly occurs for example in the 'borallyl' σ,μ-η^3-B_3H_7 ligand

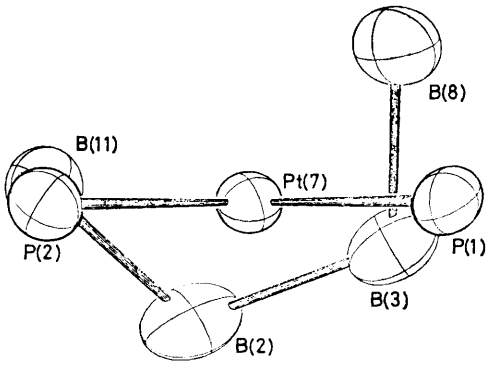

FIGURE 7 ORTEP drawing of the Pt(7)P(1)P(2)B(2)B(3)B(8)-B(11) atom system of $[7,7\text{-}(PMe_2Ph)_2\text{-}nido\text{-}7\text{-}PtB_{10}H_{12}]$, viewed normal to that plane containing P(1) and P(2) which is perpendicular to the Pt(7)P(1)P(2) plane. B(2)B(3)B(8) and B(11) are coplanar to within 0.1 pm and the B(2)B(3)B(8)B(11) plane is at a dihedral angle of 74.5° to Pt(7)P(1)P(2). The 'twist angle' θ is 21° (see Figure 8). In the 4-(2′-$B_{10}H_{13}$) derivative (Figure 3) this twist angle is 8°, B(2)B(3)B(8)B(11) are coplanar to within 0.2 pm, and the dihedral angle is nearer to 90° at 83.9°. In both compounds Pt(7)–P(1) is shortened relative to Pt(7)–P(2), and the *transoid* Pt(7)–B(11) distance appears to be correspondingly lengthened

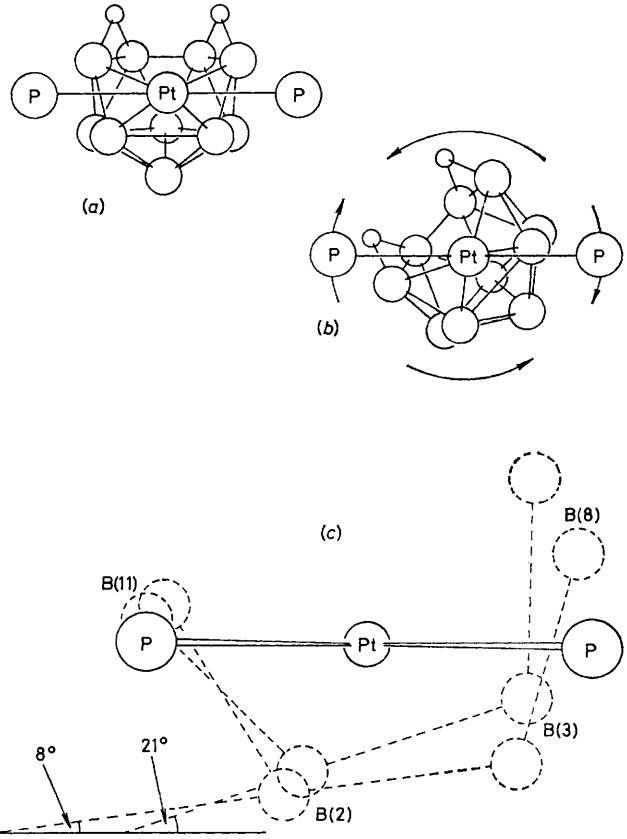

FIGURE 8 Schematic representations of (*a*) the presumed minimum-energy conformation of $[7,7\text{-}(PMe_2Ph)_2\text{-}7\text{-}PtB_{10}H_{12}]$ and (*b*) the nature of the fluxional pseudo-rotation that effectively exchanges the two phosphine ligand sites in one 180° twist; (*c*) is a superposition of drawings from the molecular structures of $[7,7\text{-}(PMe_2Ph)_2\text{-}7\text{-}PtB_{10}H_{12}]$ and its 4-(2′-$B_{10}H_{13}$) derivative which shows the initial stages of the rotation as dictated by crystal-packing forces

in $[(PMe_2Ph)_2(PtB_3H_7)]$.[31] In accord with this, the twist angle for [4-(2′-$B_{10}H_{13}$)-7,7-$(PMe_2Ph)_2$-7-$PtB_{10}H_{11}$] (Figure 3), in which the electronic structure about the Pt atom is expected to be practically identical, but the crystal forces different, is substantially different at *ca.* 8°. Also, as discussed below, these molecules undergo a facile intramolecular pseudo-rotation about the Pt atoms, of which these twist distortions will represent the initial stages. The ground-state equilibrium conformation of the P_2PtB_{10} atoms in these compounds is therefore probably that of local C_s symmetry [see Figure 8(*a*)].

As just mentioned, the molecular structure of the $[(PMe_2Ph)_2(PtB_{20}H_{24})]$ compound derived from 2,2′-$(B_{10}H_{13})_2$ is represented by the ORTEP drawing of Figure 3. Atomic co-ordinates are in the Experimental section, and selected interatomic distances and angles between interatomic vectors in Tables 5 and 6 respectively. The gross structure is seen to be similar to that of [7,7-$(PMe_2Ph)_2$-*nido*-7-$PtB_{10}H_{12}$] (Figure 1), but with a pendant 2′-$B_{10}H_{13}$ group in the 4-position. Hydrogen atoms were not located but bridging H atoms in the (8,9), (10,11), (5′,6′; 6′,7′), and (8′,9′; 9′,10′) positions

TABLE 5

Interatomic distances (pm) for [4-(2′-$B_{10}H_{13}$)-7,7-$(PMe_2Ph)_2$-7-$PtB_{10}H_{11}$] with estimated standard deviations in parentheses [a]

(*a*) From the platinum atom			
Pt(7)–P(1)	233.5(2)	Pt(7)–P(2)	234.1(3)
Pt(7)–B(2)	223.1(10)	Pt(7)–B(3)	223.5(9)
Pt(7)–B(11)	231.7(12)	Pt(7)–B(8)	232.5(11)
(*b*) Boron–boron [b]			
B(1)–B(2)	176.7(15)	B(1)–B(3)	177.0(16)
B(1)–B(4) *	180.5(15)	B(1)–B(6)	177.4(17)
B(1)–B(5)	179.4(18)		
B(2)–B(3)	181.3(15)		
B(2)–B(6)	177.1(18)	B(3)–B(4) *	180.2(16)
B(2)–B(11)	179.5(17)	B(3)–B(8)	179.2(14)
B(4)–B(5) *	179.1(17)	B(6)–B(5)	178.0(17)
B(4)–B(8) *	177.1(13)	B(6)–B(11)	177.4(15)
B(4)–B(9) *	180.0(15)	B(6)–B(10)	177.3(17)
B(5)–B(9)	177.9(15)	B(5)–B(10)	174.6(16)
B(8)–B(9)	183.8(17)	B(10)–B(11)	183.1(19)
B(9)–B(10)	197.0(18)		
B(4)–B(2′) *	170.7(15)		
B(1′)–B(2′) *	178.4(17)	B(1′)–B(4′)	179.7(19)
B(1′)–B(3′)	176.9(15)		
B(1′)–B(5′)	175.0(17)	B(1′)–B(10′)	177.3(18)
B(2′)–B(3′) *	179.3(14)	B(3′)–B(4′)	176.8(19)
B(2′)–B(5′) *	178.4(18)	B(4′)–B(10′)	180.9(20)
B(2′)–B(6′) *	173.9(17)	B(4′)–B(9′)	173.5(19)
B(2′)–B(7′) *	180.5(18)	B(4′)–B(8′)	175.6(23)
B(3′)–B(7′)	173.6(18)	B(3′)–B(8′)	176.1(19)
B(5′)–B(6′)	174.0(22)	B(9′)–B(10′)	175.6(21)
B(5′)–B(10′)	199.4(19)		
B(6′)–B(7′)	176.9(18)	B(8′)–B(9′)	178.2(21)
B(7′)–B(8′)	199.8(19)		
(*c*) Other			
P–C	181.1(9)—185.0(17)		
C–C	136.8(15)—142.5(16)		

[a] The columns compare pairs of distances that would be identical if the P_2PtB_{10} fragment had C_s symmetry about the Pt(7)B(1)B(5) plane, and the pendant B'_{10} fragment had C_s symmetry about the plane containing B(1′)B(3′) and the midpoints of B(5′)—B(10′) and B(7′)—B(8′). [b] An asterisk denotes distances to atoms involved in the *conjuncto*-inter-cluster link.

TABLE 6

Selected angles (°) between interatomic vectors for [4-(2′-$B_{10}H_{13}$)-7,7-$(PMe_2Ph)_2$-7-$PtB_{10}H_{11}$] with estimated standard deviations in parentheses

P(1)–Pt(7)–P(2)	95.4(1)		
P(1)–Pt(7)–B(2)	138.6(3)	P(2)–Pt(7)–B(3)	151.2(3)
P(1)–Pt(7)–B(3)	97.3(3)	P(2)–Pt(7)–B(2)	107.6(3)
P(1)–Pt(7)–B(8)	84.6(3)	P(2)–Pt(7)–B(11)	86.9(3)
P(1)–Pt(7)–B(11)	171.5(3)	P(2)–Pt(7)–B(8)	160.9(2)
B(2)–Pt(7)–B(3)	47.9(4)		
B(2)–Pt(7)–B(8)	83.1(4)	B(3)–Pt(7)–B(11)	83.4(4)
B(2)–Pt(7)–B(11)	46.5(4)	B(3)–Pt(7)–B(8)	46.2(3)
B(8)–Pt(7)–B(11)	89.8(4)		

are reasonably inferred from the ^1H-{^{11}B} n.m.r. spectra as discussed above. Its formulation as [4-(2′-*nido*-$B_{10}H_{13}$)-7,7-$(PMe_2Ph)_2$-*nido*-7-$PtB_{10}H_{11}$] is thus confirmed.

The heavier atoms were not located with such accuracy as for $[(PMe_2Ph)_2(PtB_{10}H_{12})]$, but within the two P_2Pt-B_{10} clusters the interatomic distances do not differ significantly between the compounds, the principal difference being in the 'twist' angle about the Pt atom discussed above (which is only 8° for the icosaboranyl derivative) together with the associated Pt–P bond lengths. Similarly the 4-(2′-*nido*-decaboranyl) cluster is near-identical to that of 2,2′-$(B_{10}H_{13})_2$ itself,[4,6] and the B(4)–B(2′) intercluster linkage of 170.7(15) pm is also the same within experimental error as that found for 2,2′-$(B_{10}H_{13})_2$ [169.2(3) pm] [4,6] and is also comparable to that in the other $B_{20}H_{26}$ isomers 2,6′-$(B_{10}H_{13})_2$ [167.9(3) pm] [6] and 1,5-$(B_{10}H_{13})_2$ [169.8(3) pm].[5] Interestingly there appeared to be no significant lengthening of *intra*-cluster distances to the B(4) and B(2′) atoms involved in the *inter*-cluster linkages. This is in contrast to the unsubstituted $(B_{10}H_{13})_2$ isomers,[5,6] which exhibit lengthenings of *ca.* 1.5 pm compared to unsubstituted $B_{10}H_{14}$, but in the present case any effects may be obscured by the limited accuracy of the data. The mutual perturbation of the two clusters *via* the B(4)–B(2′) linkage in any event appears to be rather small.

Two rotamer effects should also be mentioned. First, the rotamer conformation about the B(4)–B(2′) intercluster bond may be defined with respect to an eclipsed conformation of the B(4)–B(8) and B(2′)–B(6′) vectors and is 52°. In the parent compound 2,2′-$(B_{10}H_{13})_2$ it is 118° in the solid state.[6] Secondly, the two PMe_2Ph ligands in $[(PMe_2Ph)_2(PtB_{10}H_{12})]$ are in the commonly found configuration which has a *transoid* disposition of the bulkier phenyl groups (Figure 1). In the [$(B_{10}H_{13})$-$(PMe_2Ph)(PtB_{10}H_{11})$] compound, however (Figure 3), the much less favoured *gauche-oid* disposition is adopted.

Intramolecular Pseudo-rotation.—On heating a C_6D_6 solution of $[(PMe_2Ph)_2(PtB_{10}H_{12})]$ the two *P*-methyl ^1H n.m.r. resonance patterns (Figure 2) broaden, coalesce, then at higher temperatures become one central $[AX_n]_2$-type pattern with ^{195}Pt satellites; under ^{31}P(broad-band) decoupling this appears as a singlet central resonance with singlet ^{195}Pt satellites.[10] This implies that the chemical inequivalence of the two *P*-methyl groups on

each of the two phosphine ligands is removed by effective site exchange. This cannot occur *via* Pt–P bond dissociation since the satellite structure arising from the coupling $^3J(^{195}Pt-^1H)$ is retained. The 2 : 2 : 2 : 2 : 1 : 1 intensity ratios for the resonances in the ^{11}B n.m.r. spectrum [18] are also retained at these higher temperatures, as are the satellite structures in the $^1H-\{^{11}B\}$ and ^{11}B spectra arising from the various specific couplings $^1J(^{195}Pt-^{11}B)$, $^2J(^{195}Pt-B-^1H)$, and $^3J(^{195}Pt-B-B-^1H)$ within the platinaundecaborane cluster.[18] This indicates that the site exchange does not involve the dissociation of Pt–B bonds and also that the Pt atom is associated with the same four B(2)B(3)B(8)B(11) atoms throughout.

The most plausible mechanism for the site exchange is therefore that of a complete mutual pseudo-rotation of the η^4-$B_{10}H_{12}$ and the $(PMe_2Ph)_2$ ligands about the Pt atom as depicted in Figure 8(*b*), the initial stages of the rotation being so readily allowed that they may be induced by crystal-packing forces, as seen from the results of *X*-ray diffraction analysis [Figures 7 and 8(*c*)]. This rotation has similarities to η^4-*cis*-butadiene ligand pseudo-rotation in such complexes as *arachno*-$[(CO)_3(FeC_4H_8)]$,[33,34] and its origins probably reside in a near-cylindrically symmetrical hybrid of the three platinum–borane cluster bonding pairs that are required by a *nido*-electron count. These are presumably those in two of the dsp^2 tetragonal orbitals expected for Pt^{II} plus the lone pair in the (formal) platinum d_{z^2} orbital or a *dp* hybrid of similar symmetry. In any event the behaviour contrasts to that in [6,6,9,9-$(PMe_2Ph)_4$-*arachno*-6,9-$Pt_2B_8H_{10}$] [numbering as in (II)],[14] which does not exhibit fluxionality, and in which the d_{z^2} or *dp* hybrid lone pair is believed to bind rigidly and specifically to B(3) *via* an otherwise vacant B(3) orbital.

This type of borane ligand pseudo-rotation has not been observed to date in other similar systems, although the recently reported [35] n.m.r. behaviour of [9,9,9-$(AsMe_2Ph)_3$-*nido*-9,7,8-$RhC_2B_8H_{11}$] indicates that this compound may exhibit it, and η^5-borane to metal coordination in *closo*-species also exhibits a similar pseudo-rotation; [36] the latter, however, has closer parallels to $C_5H_5^-$ ligand behaviour which is well documented. These types of rotational non-rigidity contrast to the dynamic behaviour observed in the ostensibly similar compounds such as [2,7-Me_2-9,9-$(PEt_3)_2$-*nido*-2,7,9-$C_2PtB_7H_7$], which involve metal migration between two equivalent η^4-bonding sites; [37] this mechanism cannot apply to our compounds since the alternative bonding sites are already occupied by the bridging H(8,9) and H(10,11) atoms.

The separation of the two *P*-methyl resonances in C_6D_6 solution at ambient temperature (Table 1) together with a coalescence temperature of 71.5 °C in the 100-MHz $^1H-\{^{31}P\}$ spectrum imply an activation energy $\Delta G^{\ddagger} = 79 \pm 5$ kJ mol^{-1} for the fluxional process in $[(PMe_2Ph)_2(PtB_{10}H_{12})]$.[10] Errors in this estimation could arise from changes in Pt–P and P–C bond rotamer populations together with changing anisotropic solvent effects as the temperature increases. However, the analogous separation in $[(PMe_2Ph)_4(Pt_2B_8H_{10})]$, which exhibits similar solvent shielding effects,[14] and which will have similar steric requirements for its PMe_2Ph ligands, but which does not exhibit fluxionality, only changes from 8.8(5) Hz at 21 °C to 7.8(5) Hz at 85 °C (100-MHz spectrum; C_6D_6 solution), this suggests the figure of *ca.* 80 kJ mol^{-1} is therefore not seriously in error. A similar coalescence is also observable for the various $[(B_{10}H_{13})(PMe_2Ph)_2(PtB_{10}H_{11})]$ platinahenicosaboranes reported here, but in these cases the overlapping coalescence of 12 resonance lines (*e.g.* Figure 5) to produce six rendered the precise determination of coalescence temperatures difficult. However, derived activation energies $\Delta G^{\ddagger}_{T_c}$ were also of the order of *ca.* 80 kJ mol^{-1} for these compounds, implying no serious inhibition of the rotational process by the introduction of the decaboranyl substituents. This value is somewhat higher than the activation energies $\Delta G^{\ddagger}_{T_c}$ for iron(0)–butadiene derivatives [34] which lie in the range 25—50 kJ mol^{-1}. There seem to be few, if any, examples of butadiene ligand fluxionality in the platinum group, however; the compound $[Pd(Me_2C{=}CH{-}CH{=}CMe_2)Cl]^-$ is fluxional with $\Delta G^{\ddagger}_{T_c} = 54.4$ kJ mol^{-1} but here a hemi-dissociative π–σ–π rearrangement is postulated: [38] this involves intraligand C–C bond rotation, clearly a different process from that involved in the platinaundecaborane clusters. Ethylenic-type ligand rotation is however well known in platinum chemistry, and commonly has activation energies within the range 50—70 kJ mol^{-1} in square-planar platinum(II) complexes.[39] However, this type of ligation would be more closely parallelled in η^2-borane–metal compounds such as $[Pt(B_5H_8)Me(PMe_2Ph)_2]$ [12,19] but we have not yet investigated these for this type of rotational behaviour.

EXPERIMENTAL

General.—Reactions were generally carried out in dry solvents under an atmosphere of dry nitrogen, although in subsequent work-up and separation no particular attention was paid to maintaining strictly anaerobic conditions. All platinaborane products described here are air-stable. *NNN'N'*-Tetramethylnaphthalene-1,8-diamine, $C_{10}H_6(NMe_2)_2$, was obtained commercially, and *cis*-$[PtCl_2(PMe_2Ph)_2]$ was prepared by standard routes. *nido*-Decaborane was obtained commercially and purified by sublimation under reduced pressure. 2,2'-Bi(*nido*-decaboranyl), 2,6'-bi(*nido*-decaboranyl), and 1,5'-bi(*nido*-decaboranyl) were prepared from *nido*-decaborane, and also purified, as described elsewhere.[6,8] General chromatographic techniques were also as described elsewhere: [8,14] analytical and preparative thin-layer chromatography (t.l.c.) was carried out using Kieselgel 60G (Merck) as the stationary phase and column chromatography using Kieselgel 60 (0.063—0.200 mm mesh, Merck) as the stationary phase; columns were generally of dimensions *ca.* 25 cm × 10 cm^2. Except where specifically mentioned below, all chromatography was carried out using CH_2Cl_2–light petroleum (b.p. 60—80 °C) (50 : 50) as eluting medium. 100-MHz ^1H, 40-MHz ^{31}P, and 32-MHz ^{11}B n.m.r. spectroscopy was carried out using a JEOL FX-100 pulse (Fourier-transform) spectrometer at Leeds; 64-MHz ^{11}B spectro-

scopy was carried out on a 200-MHz Bruker instrument at the Institüt für Anorganische Chemie, University of München; the techniques of 'partial relaxation' and selective multiple resonance as applied in this work have been adequately described already.[14,18,23]

Preparation of Compounds from Reactions of cis-$[PtCl_2(PMe_2Ph)_2]$.—(*a*) *With* $K[B_{10}H_{13}]$. To a stirred solution of $B_{10}H_{14}$ (0.244 g, 2 mmol) in tetrahydrofuran (thf) (20 cm^3) maintained at 0 °C was added KH (75% active, 0.106 g, corresponding to 2 mmol KH). Immediate effervescence together with a yellow colouration occurred. After 0.5 h a solution of *cis*-$[PtCl_2(PMe_2Ph)_2]$ (0.542 g, 1 mmol) in CH_2Cl_2 (20 cm^3) was added. After 2 h, during which time the colour had darkened considerably, t.l.c. analysis showed the presence of two major components (R_f 0.7 and 0.3). The solution was filtered and the precipitate (identified as KCl) washed repeatedly with CH_2Cl_2 until the run-off was colourless. The most volatile components of the combined liquid phases were removed under reduced pressure and column chromatography then yielded $B_{10}H_{14}$ (0.105 g, 1.03 mmol; 52% recovery; t.l.c. R_f 0.7) as colourless crystals (m.p. 98—99 °C) and [7,7-$(PMe_2Ph)_2$-*nido*-7-$PtB_{10}H_{12}$] as an intensely yellow solid [t.l.c. R_f 0.3, m.p. 197—199 °C (decomp.)]. Recrystallisation of the latter from CH_2Cl_2 yielded golden yellow crystalline blocks, m.p. 197—199 °C (decomp.) (0.325 g, *ca.* 27% based on initial total $B_{10}H_{14}$) (Found: C, 32.3; H, 5.7; B, 18.5; P, 10.7. $C_{16}H_{34}B_{10}P_2Pt$ requires C, 32.5; H, 5.8; B, 18.3; P, 10.5%). One of the crystals was found suitable for *X*-ray diffraction experiments as described below.

(*b*) *With* $B_{10}H_{14}$ *and* $C_{10}H_6(NMe_2)_2$. The compound $C_{10}H_6(NMe_2)_2$ (0.43 g, 2 mmol) was added to a stirred solution of $B_{10}H_{14}$ (0.244 g, 2 mmol) in CH_2Cl_2–Et_2O (50 : 50, 50 cm^3) at ambient temperature. A yellow colouration developed immediately. After 0.3 h, *cis*-$[PtCl_2(PMe_2Ph)_2]$ (1.084 g, 2 mmol) was added and stirring continued until dissolution was complete. Over 2 h the solution darkened considerably and t.l.c. analysis then showed the presence of three components at R_f = 0.7 ($B_{10}H_{14}$), 0.3 {[$(PMe_2Ph)_2$-$(PtB_{10}H_{12})$]}, and 0.03 {*cis*-$[PtCl_2(PMe_2Ph)_2]$}. Column chromatography then yielded $B_{10}H_{14}$ (0.11 g, 54% recovery) and pure [7,7-$(PMe_2Ph)_2$-*nido*-7-$PtB_{10}H_{12}$] (0.320 g, *ca.* 26% based on $B_{10}H_{14}$). A similar procedure using a 1 : 1 : 2 (rather than a 1 : 1 : 1) ratio of reactants, *viz.* $B_{10}H_{14}$ (0.122 g, 1 mmol), $C_{10}H_6(NMe_2)_2$ (0.426 g, 2 mmol), and *cis*-$[PtCl_2(PMe_2Ph)_2]$ (0.542 g, 1 mmol) yielded [$(PMe_2Ph)_2(PtB_{10}H_{12})$] in a much greater yield based on $B_{10}H_{14}$ (*i.e.* 0.330 g, 0.57 mmol, 57%).

(*c*) *With* 2,2′-$(B_{10}H_{13})_2$ *and* $C_{10}H_6(NMe_2)_2$ *in a* 1 : 1 : 2 *molar ratio*. The compound $C_{10}H_6(NMe_2)_2$ (0.213 g, 1 mmol) was added to a stirred solution of 2,2′-$(B_{10}H_{13})_2$ (0.122 g, 0.5 mmol) in CH_2Cl_2–Et_2O (50 : 50, 50 cm^3) at ambient temperature. An immediate yellow colouration developed and after 0.25 h $[PtCl_2(PMe_2Ph)_2]$ (0.271 g, 0.5 mmol) was added. After this had dissolved the solution was allowed to stand for 5 h. T.l.c. analysis showed three components at R_f = 0.55, 0.06, and 0.04. The solution was filtered and concentrated under reduced pressure. Preparative t.l.c. yielded three components as bright yellow solids: (1) (R_f 0.55), 0.145 g, m.p. 194—199 °C (decomp.); (2) (R_f 0.06), 0.030 g, m.p. 165—175 °C (decomp.); and (3) (R_f 0.04), 0.010 g, m.p. 155—170 °C (decomp.). Components (2) and (3) were found to be identical to the isomers of [{$(PMe_2Ph)_2(PtB_{10}H_{11})$}$_2$] described in the next experiment. Component (1) was recrystallised from CH_2Cl_2 ($\leqslant$3 cm^3) to yield pure [4-(2′-$B_{10}H_{13}$)-7,7-$(PMe_2Ph)_2$-*nido*-7-$PtB_{10}H_{11}$] as yellow crystals (Found: C, 27.6; H, 6.35; B, 30.0; P, 8.8%; M = 704. $C_{16}H_{46}B_{20}P_2Pt$ requires C, 27.0; H, 6.5; B, 30.4; P, 8.7%; M = 712). One of the crystals was suitable for analysis by *X*-ray diffraction experiments as described below. The yield of (1) was 41% based on 2,2′-$(B_{10}H_{13})_2$.

(*d*) *With* 2,2′-$(B_{10}H_{13})_2$ *and* $C_{10}H_6(NMe_2)_2$ *in a* 2 : 1 : 4 *molar ratio*. To a stirred solution of 2,2′-$(B_{10}H_{13})_2$ (0.122 g, 0.5 mmol) in 1,1,2,2-$C_2H_2Cl_4$–thf (75 : 25, 50 cm^3) was added $C_{10}H_6(NMe_2)_2$ (0.428 g, 2 mmol). An immediate yellow colouration developed together with a marked turbidity. After 1 h, *cis*-$[PtCl_2(PMe_2Ph)_2]$ (0.542 g, 1 mmol) was added and stirring continued until dissolution was complete. After 24 h, t.l.c. analysis (using 100% CH_2Cl_2 as eluting medium) showed three components at R_f 0.85, 0.40, and 0.30 which corresponded to (1), (2), and (3) respectively (previous experiment) and which had approximate relative concentrations of 1 : 2 : 1. After another 24 h a flocculent yellow precipitate had developed, and the three components were present in approximate ratio of 1 : 5 : 3 respectively. The solution was filtered and concentrated under reduced pressure. Preparative t.l.c. (100% CH_2Cl_2 as liquid phase) was used to separate the components. Component (1) was identified as [4-(2′-$B_{10}H_{13}$)-7,7-$(PMe_2Ph)_2$-*nido*-7-$PtB_{10}H_{11}$] (see above) (0.031 g, 0.04 mmol, 8%) (Found: C, 27.6; H, 6.4; B, 30.1; P, 8.5%). Components (2) and (3) were tentatively identified as *cisoid*-4,6′-[$(PMe_2Ph)_2(PtB_{10}H_{11})$]$_2$ [schematic structure (IV)] and *transoid*-4,4′-[$(PMe_2Ph)_2(PtB_{10}H_{11})$]$_2$ [schematic structure (V)], and had properties as follows. Component (2): deep yellow crystals (from CH_2Cl_2), m.p. 175—180 °C (decomp.); 0.153 g, 0.13 mmol, 26% (Found: C, 31.6; H, 5.6; B, 18.3; P, 10.5%; M = 1 037). Component (3): yellow powder (from CH_2Cl_2–hexane), m.p. 158—170 °C (decomp.); 0.063 g, 0.05 mmol, 11% (Found: C, 32.2; H, 5.7; B, 17.7; P, 10.7%; M = 1 015. $C_{32}H_{66}B_{20}P_4Pt_2$ requires C, 32.5; H, 5.6; B, 18.3; P, 10.5%; M = 1 180). Each exhibited two near-coincident ^{31}P n.m.r. resonances at $\delta(^{31}P)$ = *ca.* +1 p.p.m. flanked by satellites arising from $^1J(^{195}Pt-^{31}P)$ = *ca.* 2 550 and 2 500 Hz, with $^2J(^{31}P-^{31}P)$ = *ca.* 30 Hz ($C_2H_2Cl_4$ solution).

(*e*) *With* 2,6′-$(B_{10}H_{13})_2$ *and* $C_{10}H_6(NMe_2)_2$. The compound $C_{10}H_6(NMe_2)_2$ (0.214 g, 1 mmol) was added to a stirred solution of 2,6′-$(B_{10}H_{13})_2$ (0.122 g, 0.5 mmol) in CH_2Cl_2–light petroleum (b.p. 60—80 °C) (50 : 50, 50 cm^3), whereupon an immediate yellow colour developed. The compound *cis*-$[PtCl_2(PMe_2Ph)_2]$ (0.272 g, 0.5 mmol) was added and dissolved by stirring. After 5 h, t.l.c. analysis revealed two principal components at R_f 0.65 and 0.30. The solution was filtered from the small quantity of off-white precipitate and reduced in volume under low pressure. Preparative t.l.c. isolated the two components which were identified as [7,7-$(PMe_2Ph)_2$-*nido*-7-$PtB_{10}H_{12}$] (see above) and [4-(6′-$B_{10}H_{13}$)-7,7-$(PMe_2Ph)_2$-*nido*-7-$PtB_{10}H_{11}$], having properties as follows. [$(PMe_2Ph)_2(PtB_{10}H_{12})$]: yellow crystals (from CH_2Cl_2–light petroleum), m.p. 197—199 °C (decomp.); 0.031 g, 0.05 mmol, 6% (Found: C, 31.8; H, 5.9; B, 18.1; P, 10.9%). [$(B_{10}H_{13})(PMe_2Ph)_2(PtB_{10}H_{11})$]: yellow crystalline powder (from CH_2Cl_2–light petroleum), m.p. 201—211 °C (decomp.); 0.143 g, 0.2 mmol, 41% (Found: C, 27.9; H, 6.8; B, 29.3; P, 8.2%; M = 701. $C_{16}H_{46}B_{20}P_2Pt$ requires C, 27.0; H, 6.5; B, 30.4; P, 8.7%; M = 713). Other properties are presented and discussed in the text.

(*f*) *With* 1,5′-$(B_{10}H_{13})_2$ *and* $C_{10}H_6(NMe_2)_2$. An immediate yellow colour developed when $C_{10}H_6(NMe_2)_2$ (0.214 g, 1

TABLE 7

Atomic co-ordinates for [7,7-$(PMe_2Ph)_2$-*nido*-7-$PtB_{10}H_{12}$] with estimated standard deviations in parentheses

(*a*) Non-hydrogen atoms

Atom	*x*	*y*	*z*
B(1)	0.181 4(4)	0.086 4(4)	0.320 1(5)
B(2)	0.126 5(4)	0.183 8(4)	0.275 8(4)
B(3)	0.227 5(4)	0.137 9(4)	0.203 9(5)
B(4)	0.210 6(5)	0.027 2(4)	0.203 4(6)
B(5)	0.098 9(5)	0.007 2(4)	0.266 2(5)
B(6)	0.051 5(5)	0.101 1(4)	0.321 1(5)
Pt(7)	0.123 49(1)	0.217 46(1)	0.092 64(1)
B(8)	0.184 7(4)	0.083 8(4)	0.076 6(5)
B(9)	0.100 1(5)	0.002 5(4)	0.117 0(6)
B(10)	−0.008 1(4)	0.051 4(4)	0.198 7(5)
B(11)	0.007 8(4)	0.167 2(4)	0.208 2(4)
P(1)	0.232 57(8)	0.265 37(8)	−0.033 61(9)
P(2)	−0.005 50(8)	0.308 97(7)	0.029 19(9)
C(1)	0.188 8(3)	0.258 6(3)	−0.182 6(3)
C(2)	0.122 0(4)	0.195 0(4)	−0.218 3(4)
C(3)	0.088 5(4)	0.187 8(5)	−0.332 3(5)
C(4)	0.117 6(4)	0.244 8(6)	−0.408 9(5)
C(5)	0.183 8(4)	0.308 3(4)	−0.377 1(5)
C(6)	0.219 2(3)	0.315 0(3)	−0.263 4(4)
C(7)	0.355 0(4)	0.217 4(5)	−0.026 7(6)
C(8)	0.263 8(6)	0.376 5(4)	−0.005 1(6)
C(9)	−0.110 8(4)	0.249 3(4)	−0.032 2(6)
C(10)	0.005 9(5)	0.388 1(4)	−0.081 6(5)
C(11)	−0.046 2(3)	0.373 9(3)	0.143 7(4)
C(12)	−0.144 5(4)	0.396 1(3)	0.151 9(5)
C(13)	−0.168 0(5)	0.448 7(4)	0.240 5(6)
C(14)	−0.097 1(6)	0.479 6(4)	0.317 8(5)
C(15)	−0.000 3(5)	0.459 0(4)	0.310 7(5)
C(16)	0.024 5(4)	0.405 8(3)	0.223 8(5)

(*b*) Hydrogen atoms

Atom	*x*	*y*	*z*	*U*
H(1)	0.227(4)	0.080(4)	0.397(5)	0.099(19)
H(2)	0.144(3)	0.247(3)	0.327(4)	0.058(13)
H(3)	0.306(4)	0.158(4)	0.211(5)	0.092(17)
H(4)	0.270(4)	−0.022(4)	0.204(5)	0.088(17)
H(5)	0.085(3)	−0.053(3)	0.296(4)	0.070(15)
H(6)	0.017(3)	0.099(3)	0.407(4)	0.060(13)
H(8)	0.217(3)	0.074(3)	0.009(4)	0.052(14)
H(9)	0.081(3)	−0.055(3)	0.067(4)	0.053(12)
H(10)	−0.081(3)	0.018(3)	0.194(3)	0.040(11)
H(11)	−0.049(4)	0.203(3)	0.217(4)	0.055(14)
H(10,11)	−0.009(4)	0.116(4)	0.131(4)	0.076(16)
H(8,9)	0.097(3)	0.061(3)	0.050(4)	0.046(11)
H(2)	0.102(3)	0.151(3)	−0.166(4)	0.060(14)
H(3)	0.051(5)	0.135(4)	−0.356(6)	0.112(24)
H(4)	0.103(5)	0.247(5)	−0.477(7)	0.090(21)
H(5)	0.202(3)	0.348(3)	−0.437(4)	0.055(13)
H(6)	0.265(3)	0.361(3)	−0.242(3)	0.036(11)
H(71)	0.395(4)	0.241(4)	−0.076(5)	0.079(19)
H(72)	0.351(5)	0.149(5)	−0.034(6)	0.112(25)
H(73)	0.383(4)	0.208(3)	0.048(6)	0.082(19)
H(81)	0.211(7)	0.416(6)	−0.027(8)	0.180(41)
H(82)	0.293(5)	0.378(5)	0.065(6)	0.107(25)
H(83)	0.322(4)	0.397(3)	−0.043(4)	0.071(16)
H(91)	−0.162(4)	0.283(3)	−0.071(5)	0.072(17)
H(92)	−0.130(5)	0.209(4)	0.022(6)	0.093(22)
H(93)	−0.096(5)	0.222(4)	−0.087(6)	0.073(22)
H(101)	−0.055(4)	0.415(4)	−0.100(4)	0.069(16)
H(102)	0.025(3)	0.363(3)	−0.138(4)	0.053(16)
H(103)	0.051(4)	0.427(4)	−0.056(5)	0.078(20)
H(12)	−0.191(3)	0.374(3)	0.097(4)	0.046(13)
H(13)	−0.225(4)	0.459(3)	0.248(4)	0.062(17)
H(14)	−0.113(4)	0.517(5)	0.385(5)	0.102(21)
H(15)	0.051(4)	0.483(4)	0.377(5)	0.098(20)
H(16)	0.087(4)	0.390(4)	0.221(5)	0.077(18)

mmol) was added to a stirred solution of 1,5′-$(B_{10}H_{13})_2$ (0.122 g, 0.5 mmol) in CH_2Cl_2 (50 cm^3). The compound *cis*-[$PtCl_2(PMe_2Ph)_2$] (0.272 g, 0.5 mmol) was then dissolved in the solution, which was left for 8 h, during which time it became darker in colour and a slight flocculent precipitate developed. Analytical t.l.c. revealed four yellow components, R_f 0.63, 0.55, 0.47, and 0.30, which were subjected to preparative t.l.c. as described above. This yielded [$(PMe_2Ph)_2(PtB_{10}H_{12})$] [$R_f$ 0.30; 0.035 g, 0.06 mmol, 12%; m.p. 197—199 °C (decomp.)] but the three other components could not be separated satisfactorily. Their ^{31}P and ^{11}B n.m.r. properties were grossly similar to those for [4-(6′-$B_{10}H_{13}$)-7,7-$(PMe_2Ph)_2$-7-$PtB_{10}H_{11}$] and [4-(2′-$B_{10}H_{13}$)-7,7-$(PMe_2Ph)_2$-7-$PtB_{10}H_{11}$] and so they were tentatively identified as three further isomers of [$(B_{10}H_{13})(PMe_2Ph)_2(PtB_{10}H_{11})$] as discussed in the text; their combined yield (as a yellow powder from CH_2Cl_2–light petroleum) was 0.129 g (1.17 mmol, 35%).

X-Ray Diffraction Experiments.—Crystal data. (i) [$(PMe_2Ph)_2(PtB_{10}H_{12})$], $C_{16}H_{34}B_{10}P_2Pt$, M = 591.58, Monoclinic, a = 1.3538(3), b = 1.5770(4), c = 1.1752(2) nm, β = 94.94(2)°, U = 2.4995(9) nm^3, Z = 4, D_c = 1.572 Mg m^{-3}, $F(000)$ = 1 152, space group $P2_1/n$, Mo-K_α radiation, λ = 71.069 pm, μ(Mo-K_α) = 57.78 cm^{-1}. (ii) [$(PMe_2Ph)_2(PtB_{10}H_{11}$–$B_{10}H_{13})$], $C_{16}H_{46}B_{20}Pt$, M = 711.78, Monoclinic, a = 2.5746(10), b = 0.9541(4), c = 2.7070(6) nm, β = 101.07(3)°, U = 6.526(4) nm^3, Z = 8, D_c = 1.449 Mg m^{-3}, $F(000)$ = 2 800, space group $I2/a$, Mo-K_α radiation, λ = 71.069 pm, μ(Mo-K_α) = 44.51 cm^{-1}.

Structure determination. Measurements were made on a Syntex $P2_1$ diffractometer. Cell dimensions and their standard deviations were obtained by least-squares treat-

TABLE 8

Atomic co-ordinates for [4-(2′-*nido*-$B_{10}H_{13}$)-7,7-$(PMe_2Ph)_2$-*nido*-7-$PtB_{10}H_{11}$] with estimated standard deviations in parentheses

Atom	*x*	*y*	*z*
B(1)	0.365 7(4)	0.219 1(12)	0.150 1(5)
B(2)	0.313 4(4)	0.097 9(11)	0.147 9(5)
B(3)	0.304 6(4)	0.281 0(11)	0.162 3(4)
B(4)	0.340 6(4)	0.386 5(11)	0.125 1(4)
B(5)	0.366 9(4)	0.264 5(13)	0.086 0(5)
B(6)	0.354 6(4)	0.088 6(12)	0.102 5(5)
Pt(7)	0.230 10(1)	0.172 81(3)	0.125 87(1)
B(8)	0.270 6(4)	0.381 5(11)	0.110 1(4)
B(9)	0.309 5(4)	0.363 2(12)	0.060 1(4)
B(10)	0.320 2(5)	0.164 0(14)	0.045 7(5)
B(11)	0.286 2(4)	0.050 6(12)	0.083 9(5)
B(1′)	0.386 3(5)	0.590 3(13)	0.209 7(5)
B(2′)	0.370 5(4)	0.541 8(12)	0.144 9(4)
B(3′)	0.438 0(4)	0.558 5(13)	0.176 6(5)
B(4′)	0.449 5(6)	0.673 8(14)	0.228 7(5)
B(5′)	0.337 8(5)	0.684 3(13)	0.168 7(6)
B(6′)	0.354 2(5)	0.692 8(12)	0.109 3(5)
B(7′)	0.419 7(5)	0.628 9(14)	0.116 6(5)
B(8′)	0.470 2(5)	0.719 8(16)	0.172 7(6)
B(9′)	0.445 3(5)	0.848 0(13)	0.210 0(5)
B(10′)	0.388 6(5)	0.770 9(14)	0.225 4(5)
P(1)	0.171 27(8)	0.317 70(25)	0.157 76(8)
P(2)	0.175 21(9)	−0.024 76(28)	0.114 15(12)
C(1)	0.126 5(3)	0.422 5(9)	0.112 7(3)
C(2)	0.132 2(4)	0.428 1(11)	0.063 0(4)
C(3)	0.097 0(4)	0.504 1(13)	0.027 4(4)
C(4)	0.055 3(4)	0.577 4(12)	0.043 1(5)
C(5)	0.050 2(4)	0.573 4(12)	0.093 2(5)
C(6)	0.084 7(4)	0.497 9(12)	0.127 9(4)
C(7)	0.127 8(4)	0.232 4(11)	0.195 6(3)
C(8)	0.204 6(4)	0.445 9(11)	0.204 4(4)
C(9)	0.180 3(5)	−0.154 1(13)	0.064 4(7)
C(10)	0.189 2(5)	−0.128 5(14)	0.171 7(6)
C(11)	0.103 3(3)	0.001 3(10)	0.100 3(4)
C(12)	0.084 0(4)	0.093 6(13)	0.061 0(4)
C(13)	0.028 3(5)	0.115 2(15)	0.047 3(5)
C(14)	−0.004 7(4)	0.041 9(16)	0.072 6(5)
C(15)	0.015 1(4)	−0.050 2(14)	0.111 9(5)
C(16)	0.070 1(4)	−0.070 1(11)	0.126 5(5)

ment of the setting angles of, for each compound, 15 reflections with $35 < 2\theta < 40°$. For (i) intensities of all independent reflections with $4 < 2\theta < 45°$ were measured with scan speeds, depending on intensity, between 1 and 29° min^{-1}. For (ii) all independent reflections with $4 < 2\theta < 50°$ were measured with scan speeds of 4—29° min^{-1}. The structure analysis of (i) used the 3 012 reflections with $I > 3\sigma(I)$, with 431 others below this threshold excluded, for (ii) the corresponding numbers were 4 436 and 1 354. Lorentz, polarisation, and absorption factors were calculated, and after structure solution using Patterson and electron-density syntheses, full-matrix least-squares refinement with anisotropic temperature factors converged at $R = 0.029$, $R' = 0.045$ for (i) and $R = 0.033$, $R' = 0.056$ for (ii). For (i) only, the hydrogen atoms were then located and included in the refinement, first as fixed contributions and then refined, with satisfactory convergence, to $R = 0.020$, $R' = 0.030$. Least-squares weights were derived from the variances $\sigma^2(I) = \sigma_c^2(I) + (QI)^2$, where σ_c^2 is the value from counting statistics, and the empirical factor was 0.02 for (i) and 0.03 for (ii). Atomic scattering factors were calculated from the analytical approximation and coefficients given in ref. 40, those for hydrogen being the bonded atom values.[41] The atomic co-ordinates and their standard deviations are given in Tables 7 and 8. Vibrational parameters and observed and calculated structure factors are in Supplementary Publication No. SUP 23135 (53 pp.).*

We thank the S.R.C. for support, Mr. A. Hedley for microanalyses, the University of Leeds for the award of a Student Demonstratorship (to S. K. B.) and for travel grants, and Dr. B. Wrackmeyer (Munich) for co-operation in conducting 64-MHz ^{11}B n.m.r. experiments.

[1/733 *Received*, 8*th May*, 1981]

* For details see Notices to Authors No. 7, *J. Chem. Soc., Dalton Trans.*, 1980, Index issue.

REFERENCES

[1] N. N. Greenwood, J. D. Kennedy, and D. Taylorson, *J. Phys. Chem.*, 1978, **82**, 623.
[2] N. N. Greenwood, J. D. Kennedy, T. R. Spalding, and D. Taylorson, *J. Chem. Soc., Dalton Trans.*, 1979, 840.
[3] S. K. Boocock, N. N. Greenwood, J. D. Kennedy, and D. Taylorson, *J. Chem. Soc., Chem. Commun.*, 1979, 16.
[4] N. N. Greenwood, J. D. Kennedy, W. S. McDonald, J. Staves, and D. Taylorson, *J. Chem. Soc., Chem. Commun.*, 1979, 17.
[5] G. M. Brown, J. W. Pinson, and L. L. Ingram, *Inorg. Chem.*, 1979, **18**, 1951.
[6] S. K. Boocock, N. N. Greenwood, J. D. Kennedy, W. S. McDonald, and J. Staves, *J. Chem. Soc., Dalton Trans.*, 1980, 790.
[7] S. K. Boocock, N. N. Greenwood, and J. D. Kennedy, *J. Chem. Res.*, 1981, (*S*) 50.
[8] S. K. Boocock, Y. M. Cheek, N. N. Greenwood, and J. D. Kennedy, *J. Chem. Soc., Dalton Trans.*, 1981, 1430.
[9] S. K. Boocock, N. N. Greenwood, M. J. Hails, J. D. Kennedy, W. S. McDonald, and J. Staves, 4th International Meeting on Boron Chemistry (Salt Lake City), IMEBORON IV, July 1979, paper No. 05.
[10] S. K. Boocock, N. N. Greenwood, and J. D. Kennedy, *J. Chem. Soc., Chem. Commun.*, 1980, 307.
[11] N. N. Greenwood, *Pure Appl. Chem.*, 1977, **49**, 791.
[12] N. N. Greenwood, J. D. Kennedy, and J. Staves, *J. Chem. Soc., Dalton Trans.*, 1978, 1146.
[13] N. N. Greenwood, M. J. Hails, J. D. Kennedy, and W. S. McDonald, *J. Chem. Soc., Chem. Commun.*, 1980, 37.
[14] S. K. Boocock, N. N. Greenwood, M. J. Hails, J. D. Kennedy, and W. S. McDonald, *J. Chem. Soc., Dalton Trans.*, 1981, 1415.
[15] R. M. Adams, *Pure Appl. Chem.*, 1972, **30**, 683.
[16] F. Klanberg, P. A. Wegner, G. W. Parshall, and E. L. Muetterties, *Inorg. Chem.*, 1968, **7**, 2072.
[17] T. Onak, H. Rosendo, G. Siwapinyoyos, R. Kubo, and L. Liauw, *Inorg. Chem.*, 1979, **18**, 2943.
[18] J. D. Kennedy and B. Wrackmeyer, *J. Magn. Reson.*, 1980, **30**, 529.
[19] J. D. Kennedy and J. Staves, *Z. Naturforsch., Teil. B*, 1979, **34**, 808.
[20] R. K. Harris, *Can. J. Chem.*, 1964, **42**, 2275.
[21] R. W. Rudolph, personal communication, July 1979.
[22] A. Allerhand, A. O. Clouse, R. R. Rietz, T. Roseberry, and R. Schaeffer, *J. Am. Chem. Soc.*, 1972, **94**, 2445.
[23] J. D. Kennedy and N. N. Greenwood, *Inorg. Chim. Acta*, 1980, **38**, 93.
[24] C. J. Frischie, *Inorg. Chem.*, 1967, **6**, 1199.
[25] L. J. Guggenberger, *J. Am. Chem. Soc.*, 1972, **94**, 114.
[26] N. N. Greenwood and J. A. Howard, *J. Chem. Soc., Dalton Trans.*, 1976, 177.
[27] A. R. Siedle, G. M. Bodner, A. R. Garber, R. F. Wright, and L. J. Todd, *J. Magn. Reson.*, 1978, **31**, 203.
[28] N. N. Greenwood, B. S. Thomas, and D. W. Waite, *J. Chem. Soc., Dalton Trans.*, 1975, 299.
[29] D. A. Thompson, T. K. Hilty, and R. W. Rudolph, *J. Am. Chem. Soc.*, 1977, **99**, 6774.
[30] M. Green, J. L. Spencer, F. G. A. Stone, and A. J. Welch, *J. Chem. Soc., Chem. Commun.*, 1974, 794.
[31] L. J. Guggenberger, A. R. Kane, and E. L. Muetterties, *J. Am. Chem. Soc.*, 1972, **94**, 5665.
[32] A. J. Welch, *J. Chem. Soc., Dalton Trans.*, 1975, 2270.
[33] J. D. Warren and R. J. Clark, *Inorg. Chem.*, 1970, **9**, 373.
[34] L. Kruczynski and J. Takats, *J. Am. Chem. Soc.*, 1974, **96**, 932.
[35] C. W. Jung and M. F. Hawthorne, *J. Am. Chem. Soc.*, 1980, **102**, 3024.
[36] T. B. Marder, R. T. Baker, J. A. Doi, and M. F. Hawthorne, unpublished results cited in ref. 35.
[37] See, for example, A. J. Welch, *J. Chem. Soc., Dalton Trans.*, 1973, 2270.
[38] J. Lucas and P. Kramer, *J. Organomet. Chem.*, 1971, **31**, 111.
[39] J. Ashley-Smith, Z. Douek, B. F. G. Johnson, and J. Lewis, *J. Chem. Soc., Dalton Trans.*, 1974, 128.
[40] 'International Tables for *X*-Ray Crystallography,' Kynoch Press, Birmingham, 1974, vol. 4.
[41] R. F. Stewart, E. R. Davidson, and W. T. Simpson, *J. Chem. Phys.*, 1959, **10**, 147.